Atmos. Chem. Phys. Discuss., 8, 13999–14032, 2008
www.atmos-chem-phys-discuss.net/8/13999/2008/

Atmospheric Chemistry and Physics Discussions

Parameterization of middle atmospheric water vapor photochemistry for high-altitude NWP and data assimilation

J. P. McCormack[1], **K. W. Hoppel**[2], **and D. E. Siskind**[1]

[1]Space Science Division, Naval Research Laboratory, Washington D.C., USA
[2]Remote Sensing Division, Naval Research Laboratory, Washington D.C., USA

Received: 4 June 2008 – Accepted: 27 June 2008 – Published: 23 July 2008

Correspondence to: J. P. McCormack (john.mccormack@nrl.navy.mil)

Published by Copernicus Publications on behalf of the European Geosciences Union.

Abstract

This report describes CHEM2D-H2O, a new parameterization of H_2O photochemical production and loss based on the CHEM2D photochemical-transport model of the middle atmosphere. This parameterization accounts for the altitude, latitude, and seasonal variations in the photochemical sources and sinks of water vapor over the pressure region from 100–0.001 hPa (~16–90 km altitude). A series of free-running NOGAPS-ALPHA forecast model simulations offers a preliminary assessment of CHEM2D-H2O performance over the June 2007 period. Results indicate that the CHEM2D-H2O parameterization improves global 10-day forecasts of upper mesospheric water vapor compared to forecasts using an existing one-dimensional (altitude only) parameterization. Most of the improvement is seen at high winter latitudes where the one-dimensional parameterization specifies photolytic H_2O loss year round despite the lack of sunlight in winter. The new CHEM2D-H2O parameterization should provide a better representation of the downwelling of dry mesospheric air into the stratospheric polar vortex in operational analyses that do not assimilate middle atmospheric H_2O measurements.

1 Introduction

Although the middle atmosphere (15–100 km altitude) is extremely dry when compared to the troposphere, detailed knowledge of the water vapor distribution in this region is important for a number of reasons. For example, water vapor abundance controls the availability of odd hydrogen species for catalytic ozone loss. In addition, the emission of longwave (terrestrial) radiation to space by water vapor is an important cooling process in the middle atmosphere. The relatively long photochemical lifetime of middle atmospheric water vapor also makes it a useful tracer for studying the dynamics of this region. Finally, the abundance of middle atmospheric water vapor is an important factor controlling the formation of both polar stratospheric clouds in winter and

ACPD

8, 13999–14032, 2008

polar mesospheric (or noctilucent) clouds near the summer mesopause, the former being important for heterogeneous ozone loss. In more practical terms, water vapor is a fundamental prognostic variable in the dynamical cores of most numerical weather prediction (NWP) models. For these reasons, NWP and data assimilation (DA) systems whose top levels extend into the upper stratosphere and mesosphere require an accurate description of the photochemical sources and sinks of water vapor.

In general, operational requirements for timely forecasts prevent NWP systems from performing fully coupled photochemical model calculations because they are too computationally intensive. One solution to this problem is to develop and employ parameterizations of the relevant photochemical processes. This report describes a new water vapor photochemistry parameterization that is based on the CHEM2D zonally averaged photochemical-transport model of the middle atmosphere. CHEM2D has been successfully used to develop fast, accurate parameterizations of stratospheric ozone photochemistry (McCormack et al., 2004, 2006). Here we apply a similar approach to provide a suitable parameterization of middle atmospheric water vapor photochemistry for operational NWP/DA systems.

This new water vapor photochemistry parameterization, designated CHEM2D-H2O, has been recently implemented in the high-altitude version of the Navy Operational Global Atmospheric Prediction System (NOGAPS-ALPHA). Here we present a description of CHEM2D-H2O as well as results from a series of NOGAPS-ALPHA forecast model simulations designed to evaluate CHEM2D-H2O and compare its performance to a simpler one-dimensional (1-D) water vapor photochemistry scheme currently used in operational NWP/DA systems. The ultimate goal of this work is to provide global simulations of mesospheric water vapor accurate enough to identify the physical processes governing polar mesospheric cloud (PMC) formation near the summer mesopause. Section 2 gives a general overview of the CHEM2D model and middle atmospheric water vapor photochemistry. Section 3 describes the implementation of CHEM2D-H2O in NOGAPS-ALPHA. Section 4 examines middle atmospheric water vapor fields from a series of NOGAPS-ALPHA forecast model simulations to assess the performance

of CHEM2D-H2O. Section 5 summarizes these results and outlines future research applications of CHEM2D-H2O.

2 H_2O photochemistry in the CHEM2D model

CHEM2D is a zonally averaged (2-D) global model that features a fully self-consistent treatment of radiative, photochemical, and dynamical processes of the middle atmosphere (see, e.g., McCormack et al., 2006; McCormack et al., 2007). The model photochemistry accounts for reactions among 54 different species using reaction rates from Sander et al. (2003). CHEM2D extends from pole to pole with grid points spaced every 4.8° in latitude; the vertical domain consists of 88 pressure levels from the surface to p=6×10^{-5} hPa (~116 km) spaced every ~1.3 km.

Water vapor (H_2O) in the middle atmosphere is produced directly through oxidation of stratospheric methane (CH_4) by the hydroxyl radical (OH + CH_4 → H_2O + CH_3) and indirectly through a series of reactions involving the methyl radical (CH_3). The net effect is that approximately two H_2O molecules are produced for each CH_4 molecule lost (e.g., LeTexier et al., 1988, and references therein). Consequently, the total number density of hydrogen throughout much of the stratosphere Q=2[CH_4] + [H_2O] is a constant (neglecting the relatively small amount of molecular hydrogen, H_2). This relationship can be used to express stratospheric H_2O production in terms of H_2O abundance, which is advantageous since it eliminates the need for a prognostic CH_4 variable.

Figure 1a plots vertical profiles of individual CHEM2D CH_4 loss rates (molecules cm^{-3} s^{-1}) at 5° N on 15 June. Reactions (5) and (6) listed in Fig. 1a are the key reactions responsible for stratospheric H_2O production. Figure 1b plots CHEM2D vertical profiles of H_2O loss rates via photolysis by solar UV and Lyman-α radiation at 5° N on 15 June. The H_2O loss rates for this latitude and month peak near 0.02 hPa (~80 km).

Photochemical loss rates are commonly used to infer an effective photochemical lifetime, which is a convenient way to quantify the relevant time scales for photochemistry relative to other physical processes such as advection. Figure 2 plots CHEM2D

ACPD
8, 13999–14032, 2008

photochemical lifetimes of CH_4 and H_2O, τ_{CH4} and τ_{H2O}, respectively, for June and December conditions throughout the middle atmosphere. The lifetimes are computed from the sum of the individual loss rates as

$$\tau_{CH4} = \frac{[CH_4]}{\sum_{i=1}^{6} L_i}, \quad \tau_{H_2O} = \frac{[H_2O]}{\sum_{i=1}^{4} L_i} \tag{1}$$

where $[CH_4]$ and $[H_2O]$ denote CHEM2D CH_4 and H_2O abundances (molecules cm^{-3}) and L_i is the loss rate (molecules cm^{-3} s^{-1}) for the individual reactions in Fig. 1.

Figure 2a and 2b show that the shortest CH_4 lifetimes (<2 days) are in the summer mesopause region where photolysis is the dominant loss mechanism. A secondary minimum in τ_{CH4} is seen near the summer polar stratopause due to rapid CH_4 loss via reaction with chlorine (Reaction 4 in Fig. 1). Based on the values of τ_{CH4} in Fig. 2a and 2b, H_2O production in the stratosphere can be considered slow compared to typical transport timescales. As a result, including the effects of this process in typical NWP/DA systems issuing 5- to 10–day forecasts is not crucial provided that accurate stratospheric humidity data are being regularly assimilated globally. In the absence of such data, or when conducting longer free-running model simulations for seasonal prediction or climate simulations, the contribution of CH_4 oxidation to H_2O production becomes more significant. Figure 2c and 2d show that values of τ_{H2O} in the summer hemisphere are less than 5 days above the 0.01 hPa level, indicating that H_2O photolysis is an important effect for accurate medium-range forecasts in this region. Values of τ_{H2O} near the mesopause increase rapidly poleward of 50° latitude in winter as the amount of sunlight diminishes.

To highlight the latitude, altitude, and seasonal dependences of H_2O photochemistry in the middle atmosphere, Fig. 3 plots the net CHEM2D photochemical tendency for water vapor, $(P-L)_{H2O}$, in parts per million by volume (ppmv) per month as a function of latitude and pressure for 15 June and 15 December, where P is the net production rate and L is the net loss rate. In the stratosphere, $(P-L)_{H2O}$ is weakly positive due to the relatively slow formation of H_2O through CH_4 oxidation (see Fig. 2) and the absence

of water vapor loss via photolysis at these altitudes (see Fig. 4). In the mesosphere, $(P-L)_{H2O}$ is mostly negative due to photolytic loss, with the largest loss rates occurring near the summer mesopause region. The positive values of $(P-L)_{H2O}$ in the winter hemisphere near 80 km poleward of 50° latitude are the result of enhanced H_2O production via the reaction $OH + HO_2 \rightarrow H_2O + O_2$. This enhancement is due to poleward transport of OH from the tropics to higher latitudes where OH becomes very long-lived in the upper mesosphere (Brasseur and Solomon, 1986).

The values of τ_{CH4}, τ_{H2O}, and $(P-L)_{H2O}$ presented in this section, which vary with latitude, altitude, and month, serve as the basis for the new CHEM2D-H_2O parameterization. CHEM2D-H_2O differs from the water vapor photochemistry parameterization currently used in the European Centre for Medium Range Weather Forecasts (ECMWF) Integrated Forecast system (IFS) (Untch and Simmons, 1999; ECMWF, 2006; Feist et al., 2007), which parameterizes production via stratospheric CH_4 oxidation and loss via mesospheric photolysis as a function of altitude only, neglecting possible latitude and seasonal dependences. This method expresses the water vapor photochemical tendency as

$$\frac{\partial r}{\partial t} = k_1(r_Q - r) - k_2 r \tag{2}$$

where r is the local water vapor mixing ratio and r_Q is the equivalent total hydrogen mixing ratio. The coefficients k_1 and k_2 are determined from analytical fits to quoted values of τ_{CH4} and τ_{H2O}, respectively, at various altitudes from Brasseur and Solomon (1986).

The coefficients k_1 and k_2 vary with altitude and are constant with latitude and season. It is assumed that r_Q has a constant value of 6.8 ppmv based on the results of Randel et al. (1998). Figure 4 plots CHEM2D values of r_Q showing this assumption holds for most of the stratosphere except winter polar regions where downward transport of dry mesospheric air occurs (LeTexier et al., 1988; Randel et al., 1998). Thus the ECMWF scheme provides a reasonable 1-D photochemical constraint on global stratospheric H_2O, but may overestimate stratospheric H_2O production in regions where

conservation of r_Q breaks down.

To illustrate the differences between this 1-D approach and the CHEM2D-H2O parameterization, Fig. 5 compares the vertical profile of the combined photochemical lifetime, $(k_1+k_2)^{-1}$ from the ECMWF scheme (ECMWF, 2006) with values of τ_{CH4} and τ_{H2O} computed with the CHEM2D model over the equator for each month of the year. Also plotted in Fig. 5 are values of the combined CHEM2D lifetime

$$\tau^* = \frac{1}{\tau_{CH4}^{-1} + \tau_{H2O}^{-1}} \quad (3)$$

for each month, which provides a single, concise description of the time scale for H_2O photochemistry throughout the middle atmosphere analogous to $(k_1+k_2)^{-1}$ in the ECMWF scheme. The overlapping curves in Fig. 5 indicate that there is virtually no seasonal dependence in the H_2O production and loss terms at low latitudes, also shown in Figs. 2 and 3. As a result, CHEM2D values of τ^* for all 12 months closely match the 1-D scheme's k_1^{-1} and k_2^{-1} values that are based on the results of Brasseur and Solomon (1986). At higher latitudes, however, Fig. 6 shows that the seasonal variations in τ_{H2O} and τ_{CH4} are both quite large.

The CHEM2D model results presented in this section demonstrate that the net middle atmospheric H_2O photochemical tendency exhibits pronounced latitude and seasonal variations that should be accounted for in NWP/DA systems extending into the mesosphere. The CHEM2D-H2O parameterization described in the following section accounts for these variations.

3 CHEM2D-H2O in NOGAPS-ALPHA

This section describes the CHEM2D-H2O parameterization and its implementation in NOGAPS-ALPHA. First, we briefly describe the NOGAPS-ALPHA forecast model and data assimilation components. We then provide a detailed description of the CHEM2D-H2O scheme as it is currently used in NOGAPS-ALPHA.

3.1 NOGAPS-ALPHA description

The high-altitude NOGAPS-ALPHA NWP/DA system (Hoppel et al., 2008) is capable of assimilating middle atmosphere constituent measurements such as H_2O profiles obtained from the NASA EOS Aura Microwave Limb Sounder (MLS) (Eckermann et al., 2008[1]). The 68-level (L68) NOGAPS-ALPHA global spectral forecast model (GSFM) initializes and advects specific humidity q at all levels from the surface to its top at 5×10^{-4} hPa. The q fields are initialized using traditional meteorological analyses from the surface up to the 200 hPa level. Above this level, the humidity fields can be initialized using either assimilated water vapor measurements for a specific date or a zonal monthly mean climatology based on measurements from the Upper Atmospheric Research Satellite (UARS) Halogen Occultation (HALOE) and MLS instruments (Randel et al., 1998; Grooß and Russell, 2005), depending on the application.

Parameterizations for moist physics in NOGAPS-ALPHA are identical to those used in the operational version of NOGAPS (Hogan and Rosmond, 1991). These include shallow cumulus mixing (Tiedtke, 1984), deep cumulus convection (Peng et al., 2004), and convective, stratiform, and boundary layer cloud formation and precipitation (Slingo, 1987; Teixeira and Hogan, 2002). For a more complete description of NOGAPS-ALPHA model physics, see McCormack et al. (2006) and (Eckermann et al., 2008[1]). Since they are designed primarily for tropospheric applications, the model's moist physics routines are only employed from the surface up to the 50 hPa level (~20 km). In the stratosphere and mesosphere, parameterized water vapor photochemical production and loss constrain the NOGAPS-ALPHA q fields. Without this photochemical constraint, upwelling of stratospheric air into the mesosphere would produce unrealistically high values of mesospheric humidity over forecast periods of

[1]Eckermann, S. D., Hoppel, K. W., Coy, L., McCormack, J. P., Siskind, D. E., Nielsen, K., Kochenash, A., Stevens, M. H., and Englert, C. R.: High-altitude data assimilation system experiments for the Northern Hemisphere summer mesosphere season of 2007, in review, J. Atmos. Sol. Terr. Phys., 2008.

2–3 days. This would pose a problem for accurate forecasts of mesospheric humidity, especially in regions where humidity measurements are not assimilated.

All forecast model results in this study employ triangular truncation of the first 79 wavenumbers (T79), giving a horizontal grid spacing of 1.5° in longitude and latitude on the quadratic Gaussian grid. The model uses the non-orographic gravity wave drag parameterization of Garcia et al. (2007) with the same settings as in Eckermann et al. (2008)[1]. The T79L68 model is initialized with analyzed winds, temperature, and constituents (e.g., O_3 and H_2O) produced by the NOGAPS-ALPHA DA component, which is described in detail by Hoppel et al. (2008) and Eckermann et al. (2008)[1]. From the surface to the mid-stratosphere, these NOGAPS-ALPHA analyses are based on assimilation of conventional meteorological data sets used by the operational T239L30 system. For the June 2007 period studied here, NOGAPS-ALPHA also assimilates EOS Aura temperature, O_3, and H_2O profiles (Froidevaux et al., 2006), as well as temperatures from the Sounding of the Atmosphere Using Broadband Radiometry (SABER) instrument on the Thermosphere Ionosphere Mesosphere Energetics and Dynamics (TIMED) satellite (Kutepov et al., 2006), up to the 0.002 hPa level, (Eckermann et al., 2008[1]). Above this level, model fields are initialized with climatology as in McCormack et al. (2006).

This report focuses exclusively on the NOGAPS-ALPHA forecast model simulations of middle atmospheric water vapor designed to test the new CHEM2D-H2O photochemistry parameterization. The following section describes the implementation of CHEM2D-H2O in NOGAPS-ALPHA.

3.2 The CHEM2D-H2O parameterization

The CHEM2D-H2O parameterization in NOGAPS-ALPHA expresses the local time rate of change of the H_2O mixing ratio r as the difference between the zonally averaged production and loss rates computed with the CHEM2D model (see Fig. 3):

$$\frac{\partial r}{\partial t} = (P - L)_{\mathrm{H2O}}. \quad (4)$$

Although specific humidity q is the NOGAPS-ALPHA model's prognostic variable, for the sake of consistency with the photochemical parameterization in Eq. (2) we will use volume mixing ratio r as the moisture variable in the following discussion. Model mixing ratio r is related to q through the relation

$$r = \frac{M_d}{M_w} \frac{q}{1-q} \tag{5}$$

where M_d and M_w are the molecular weights of dry air and H_2O, respectively.

We assume that $(P-L)_{H2O}$ is primarily a function of r. In the mesosphere, this assumption is justified because the loss rate due to photolysis is directly proportional to the local H_2O mixing ratio. In the stratosphere, where the production rates via methane oxidation depend on the local CH_4 mixing ratio, this assumption holds where the local H_2O mixing ratio can be expressed in terms of the CH_4 mixing ratio through the approximate conservation of r_Q (see Fig. 4). Where the assumption of r_Q conservation breaks down, i.e., in the winter polar stratosphere, CHEM2D values of τ_{CH4} exceed 100 days. As shown below, accounting for these latitude and seasonal variations in H_2O production and loss ensures that the CHEM2D-H2O parameterization only introduces photochemical tendencies in regions where its underlying assumptions are valid.

The function $(P-L)_{H2O}[r]$ can be approximated using a first-order Taylor series expansion about a reference state such that

$$\frac{\partial r(\lambda, \phi, p, t)}{\partial t} = (P-L)^o_{H2O} + \left.\frac{\partial (P-L)_{H2O}}{\partial r}\right|_o \left(r - r^o\right) \tag{6}$$

where λ is longitude, ϕ is latitude, p is pressure, and "o" denotes the reference state.

We proceed by assuming that Eq. (6) yields an equilibrium (reference) state r^o that is the net balance between photochemical production and loss, such that any deviations from this state can be treated as small perturbations about that reference state. This follows the method used in linearized ozone photochemistry schemes, as reviewed by McCormack et al. (2006) and Lahoz et al. (2007).

ACPD
8, 13999–14032, 2008

Applying the expansion Eq. (6) to the ECMWF relation Eq. (2), it is straightforward to show that

$$(P - L)^o_{H_2O} = k_1 \left(r_Q - r^o\right) - k_2 r^o, \tag{7}$$

$$\frac{\partial (P - L)^o_{H_2O}}{\partial r}\Big|_o = -(k_1 + k_2) \tag{8}$$

illustrating that this approach is mathematically consistent with the 1-D parameterization in Eq. (2).

As already discussed in Sect. 2 and illustrated in Figs. 5 and 6, the CHEM2D-H2O analog of Eq. (8) is

$$\frac{\partial (P - L)^o_{H_2O}}{\partial r}\Big|_o = -(\tau^*)^{-1} \tag{9}$$

where τ^* values, given by the expression Eq. (3), are tabulated as a function of latitude, pressure and season from CHEM2D model rates and then interpolated in space and time to the NOGAPS-ALPHA forecast model grid. Figure 7 plots the latitude and altitude dependence of τ^* for June and December conditions.

The analytical ECMWF expression Eq. (7) assumes constant total hydrogen r_Q=6.8 ppmv at all altitudes. As illustrated in Fig. 4, this assumption breaks down in the upper stratosphere and mesosphere. In addition, CH_4 oxidation becomes a negligible source of H_2O in the mesosphere. Thus, for CHEM2D-H2O we instead derive $(P-L)^o_{H_2O}$ values as a function of latitude, pressure and season directly from the CHEM2D model, examples of which were shown previously in Fig. 3. This approach enables us to compute equilibrium rates without any explicit reference to total hydrogen, and thus to extend these rates into the mesosphere where total hydrogen conservation breaks down and is dominated by photolytic loss.

Adopting an approach similar to that for the CHEM2D ozone photochemistry parameterization, or CHEM2D-OPP (McCormack et al., 2006), the specific humidity photochemical tendency in NOGAPS-ALPHA is applied by first defining a photochemical steady state value for the water vapor mixing ratio

$$r^{ss} = r^{o} + (P - L)^{o}\tau^{*} \tag{10}$$

so that the H_2O mixing ratio tendency can be expressed as

$$\frac{\partial r}{\partial t} = \frac{-(r - r^{ss})}{\tau^{*}}. \tag{11}$$

The updated mixing ratio value is computed using a standard backward-Euler solution of the form

$$r(t + \Delta t) = r(t) + [r^{ss} - r(t)] \left[\frac{\frac{\Delta t}{\tau^{*}}}{1 + \frac{\Delta t}{\tau^{*}}} \right] \tag{12}$$

and then converted to specific humidity using Eq. (5).

In theory, the reference state mixing ratio r^{o} should correspond to the CHEM2D model mixing ratio at photochemical equilibrium. In practice, values of $r^{o}(\phi, p, t)$ are often specified using an observation-based climatology of middle atmospheric water vapor. Based on earlier experience with linearized ozone photochemistry parameterizations (McCormack et al., 2006; Geer et al., 2007; Coy et al., 2007), use of an observation-based reference state ensures that the linearized photochemical tendency terms will not produce large biases between the modeled and assimilated constituent values, which can negatively impact forecast skill. In this study, we evaluate the performance of CHEM2D-H2O using two different r^{o} distributions. The first is based on monthly zonal mean MLS/HALOE climatology (Randel et al., 1998; Grooß and Russell, 2005) between 100–0.01 hPa combined with CHEM2D model values above the 0.01 hPa level. The second is based on monthly zonal mean NOGAPS-ALPHA analyzed H_2O for June 2007 up to the 0.002 hPa level, and CHEM2D model values above

this level. Solar UV fluxes in the CHEM2D model were set to solar minimum levels to match June 2007 conditions. Figure 8 compares these two r^o distributions. The analyzed H_2O mixing ratios are generally higher than climatological values throughout the Northern Hemisphere extratropical upper mesosphere. The results presented in the following section demonstrate how these differences impact 10-day forecasts of middle atmospheric H_2O.

4 Results

Table 1 lists three sets of NOGAPS-ALPHA forecast model simulations, designated EXP1, EXP2, and EXP3, used to demonstrate the capabilities of the new CHEM2D-H2O parameterization. EXP1 employs CHEM2D-H2O with a monthly zonal mean climatological reference state r^o for the month of June (see Fig. 8a). EXP2 employs CHEM2D-H2O with a reference state based on monthly zonal mean NOGAPS-ALPHA analyzed H_2O mixing ratios for June 2007 (Fig. 8b). EXP3 uses the 1-D water vapor photochemistry parameterization Eq. (2) currently used in the operational ECMWF IFS. These three sets of simulations each contain a series of five 10-day forecasts initialized on 5, 10, 15, 20, and 25 June 2007, encompassing the period when PMC's were observed in the Arctic region (Eckermann et al., 2008[1]).

We first examine the performance of CHEM2D-H2O using the climatological reference state (r^o) distribution (EXP1). Figure 9a plots the water vapor mixing ratio initial conditions for 00:00 UTC on 5 June 2007, which are based on the assimilation of Aura MLS Version 2.2 (V2.2) H_2O profiles between 100–0.002 hPa (~16–90 km) combined with CHEM2D model values of the H_2O above the 0.002 hPa level (see Eckermann et al., 2008[1] for details). Note that EXP1, EXP2, and EXP3 simulations all use the same sets of initial conditions.

Figure 9b plots the model H_2O mixing ratios on day 10 of the EXP1 simulation valid 15 June at 00:00 UTC. A comparison of Fig. 9b with Fig. 9a shows that the major differences in NOGAPS-ALPHA zonal mean H_2O after 10 days are: (1) a decrease at

all latitudes above the 0.01 hPa level (~82 km); (2) an increase near 0.1 hPa (~65 km) poleward of 50° N; (3) a decrease over high southern latitudes between 1.0–0.1 hPa. The high latitude changes are consistent with upwelling (downwelling) of moist (dry) air in the summer (winter) polar mesosphere. The broad decreases above the 0.01 hPa level are the result of the parameterized photolysis of H_2O.

Figure 9c plots the zonal mean NOGAPS-ALPHA analyzed H_2O mixing ratios valid on 00:00 UTC 15 June 2007. This and all following plots of analyzed H_2O extend to 0.0025 hPa, which is the closest vertical level to the 0.002 hPa upper limit for scientifically useful MLS H_2O measurements (Froidevaux et al., 2006). Since NOGAPS-ALPHA analyzed H_2O is completely constrained by the MLS measurements, the analyzed zonal mean values are essentially the same as a zonal mean estimated directly from the daily MLS data. Comparison of the analyzed H_2O with the 10-day fields from EXP1 (Fig. 9b) shows large differences poleward of 30° N above the 0.01 hPa level, where the analyzed values are much higher than the modeled values. Figure 9d plots the differences between the zonal mean analyzed H_2O and 10-day hindcast H_2O. After 10 days the EXP1 model simulation underestimates the zonal mean H_2O mixing ratio throughout the northern extratropical upper mesosphere. This is the same region where the climatological and the analysis-based r^o distributions differ substantially (Fig. 8), and where photolytic loss dominates (Fig. 3).

As mentioned in the previous section, the performance of the CHEM2D-H2O parameterization can be affected by the choice of the background reference state r^o because it relaxes the forecast model H_2O mixing ratios in the upper levels toward the reference state value r^o. In practice, the water vapor distribution used to represent r^o should be chosen so as to avoid any systematic bias between the prognostic humidity variable and the assimilated humidity fields used to initialize and update the forecast system (see, e.g. Coy et al., 2007). Systematically low values of r^o, such as those seen in Fig. 8a, can lead to an overestimate of the H_2O loss in the northern summer upper mesosphere. This may help explain why the 10-day EXP1 forecast underestimates the H_2O mixing ratio compared to the analyses (Fig. 9d) in the northern extratropical upper

mesosphere.

To investigate this possibility, we isolate the effect of parameterized water vapor photochemistry by taking the difference between the model mixing ratio r and a passive humidity tracer r_{pass}, which uses the same initial conditions as r but is not subject to parameterized photochemistry and moist physics. In the troposphere and lowermost stratosphere, the lack of moist physics in the passive humidity field produces huge differences between r and r_{pass} (not shown). In the upper stratosphere and mesosphere, differences between r and r_{pass} are due primarily to the effect of the CHEM2D-H2O parameterized photochemistry acting on r.

Figure 10 plots zonal mean values of the difference $\Delta r = r - r_{pass}$ throughout the middle atmosphere on day 10 of EXP1, EXP2, and EXP3 simulations initialized 00:00 UTC 5 June 2007. In all three simulations, the effects of the parameterized photochemistry on the model H_2O after 10 days are relegated to the upper mesosphere. Specifically, values of Δr are negative throughout the Northern Hemisphere between 0.03–0.001 hPa, consistent with H_2O loss via photolysis (e.g., Fig. 5) that peaks at high summer latitudes. The extension of negative values of Δr across the equator and into the winter hemisphere is a consequence of photochemically-processed air with lower mixing ratio r being transported from the northern summer mesosphere into the southern winter hemisphere by the mean meridional circulation. Since the timescale for H_2O production via CH_4 oxidation is >50 days in most of the stratosphere (see Fig. 5), values of Δr after 10 days in Fig. 10 are quite small throughout the stratosphere. into the southern winter hemisphere by the mean meridional circulation. Since the timescale for H_2O production via CH_4 oxidation is >50 days in most of the stratosphere (see Fig. 5), values of Δr after 10 days in Fig. 10 are quite small throughout the stratosphere.

Comparing the amount of photochemical loss among the three different simulations in Fig. 10, we find that the greatest amount of loss is produced in EXP1 using CHEM2D-H2O with climatological values of r^o (Fig. 10a). The amount of loss produced by CHEM2D-H2O is greatly reduced in EXP2 when the climatological values of r^o are replaced with values based on the June 2007 monthly zonal mean NOGAPS-ALPHA

analyzed H_2O (Fig. 10b), particularly between the 0.01 and 0.001 pressure levels. Both EXP2 and EXP3 results show similar amounts of loss in the upper mesosphere at high northern latitudes. This indicates that both CHEM2D-H2O and ECMWF parameterizations produce comparable results in the region where peak H_2O photolysis occurs. Figure 10c also indicates that the ECMWF parameterization used in EXP3 produces loss at high southern latitudes where no sunlight is present, unlike the CHEM2D-H2O results in EXP1 and EXP2.

To further characterize the performance of CHEM2D-H2O in NOGAPS-ALPHA, we compare 10-day forecast model H_2O fields with analyzed H_2O using five sets of simulations initialized 00:00 UTC on 5, 10, 15, 20, and 25 June 2007. Figure 11a plots vertical profiles of the global area-weighted mean difference between analyzed and forecast H_2O mixing ratios (denoted "A–F") from all five sets. We find that the CHEM2D-H2O parameterization with climatological r^o values in EXP1 produces the largest mean values of A–F above the 0.1 hPa level, consistent with the excessive H_2O loss seen in Fig. 10. In contrast, CHEM2D-H2O with analysis-based r^o values produces the smallest mean A–F values. This result holds true when we examine mean A–F values over separate latitude bands between 90° S–90° N (Fig. 11b–f). Figure 11 also shows that the ECMWF scheme in EXP3 produces larger values of A–F than the CHEM2D-H2O scheme in EXP2, particularly in the southern extratropics (Fig. 11b and Fig. 11c).

Overall, the combination of the CHEM2D-H2O scheme and an analysis-based reference state r^o distribution produces better forecasts of upper mesospheric H_2O than the 1-D ECMWF scheme for the June 2007 period. Much of the improvement obtained with CHEM2D-H2O is found in the high southern (winter) latitudes, where the ECMWF scheme specifies photolytic loss of H_2O year round despite the absence of sunlight during winter. At high northern (summer latitudes) CHEM2D-H2O and ECMWF H_2O results are comparable.

The preliminary evaluation of forecast model results for the June 2007 period indicates that all of the 10-day forecasts tend to underestimate the H_2O mixing ratios in the northern extratropics (see Fig. 11e) compared to the analyzed MLS values above

the 0.01 hPa level, regardless of the details of the photochemistry parameterization. It should be noted that the Aura MLS accuracy limits (±0.5 ppmv) and broad (12–16 km) vertical resolution in the upper mesopheric H_2O retrievals (Lambert et al., 2007) may complicate the evaluation of forecast skill in this region. It should also be noted that the forecast model transport in the upper mesosphere is highly sensitive to the details of the parameterized gravity wave drag, and that these details remain poorly constrained by observations. Because the effective H_2O lifetime is comparable to transport timescales in the 0.1–0.01 hPa region, deficiencies in model transport may contribute to some of the disagreement between the observations and the 10-day forecast model simulations. The effects of model transport in general, and gravity wave drag in particular, on NOGAPS-ALPHA middle atmospheric H_2O simulations are currently under investigation.

Finally, to demonstrate the effect of the CHEM2D-H2O and ECMWF photochemistry parameterizations on stratospheric water vapor, where the relevant photochemical time scales are much longer than in the mesosphere, the EXP1 and EXP3 simulations were extended out to day 90. Figure 12 compares zonal mean Δr values from EXP1 and EXP3 between 10–0.1 hPa on day 90. In general, we find that both schemes produce small increases in water vapor (0.25–0.5 ppmv) in the tropical upper stratosphere. A notable result in Fig. 12 is that the CHEM2D-H2O scheme in EXP1 leads to relatively more photochemical loss of H_2O in the mesosphere compared to the ECMWF scheme in EXP3 and thus a drier upper stratosphere over the South Pole due to downward transport of mesospheric air at high winter latitudes. This result suggests that using a H_2O photochemistry parameterization with latitude and seasonal dependences may reduce the moist bias in mesospheric H_2O seen in ECMWF analyses (Feist et al., 2007), and thereby improve its representation of dry mesospheric air descending into the polar vortex during winter and spring. To address this issue further, we plan to compare NOGAPS-ALPHA water vapor analyses from the full assimilations system using both the CHEM2D-H2O and ECMWF parameterizations over the course of the entire season.

5 Conclusions

We have described and tested the new CHEM2D-H2O parameterization for middle atmospheric water vapor photochemistry. CHEM2D-H2O is based on output from a zonally averaged (2-D) model with full photochemistry and accounts for the latitude, altitude, and seasonal dependences in the production and loss terms due to CH_4 oxidation and H_2O photolysis, respectively. The parameterization is valid up to lower thermospheric altitudes of ~95–100 km.

A series of 10-day NOGAPS-ALPHA forecast model simulations with parameterized H_2O photochemistry were performed for the June 2007 period to evaluate the model's prognostic capability for middle atmospheric H_2O. The forecast model H_2O mixing ratios were compared with NOGAPS-ALPHA analyzed H_2O fields based on assimilation of Aura MLS profile measurements. We find that the CHEM2D-H2O and ECMWF parameterizations both perform comparably at all altitudes below the 0.1 hPa level. Above this level, we find that CHEM2D-H2O performance is dependent on the choice of the reference state mixing ratio distribution. In the June 2007 case examined here, using CHEM2D-H2O with a reference state mixing ratio distribution based on the monthly zonal mean NOGAPS-ALPHA H_2O analyses for June 2007 produced better results than using a reference state based on UARS HALOE and MLS H_2O climatology spanning the 1990's. Middle atmospheric water vapor mixing ratios were lower in the early 1990's and exhibited significant positive trends during the UARS time period (e.g., Nedoluha et al., 1998; Randel et al., 1999). Therefore it is not surprising that the use of the UARS H_2O climatology to specify r^o in EXP1 leads to a systematic underprediction for the June 2007 period analyzed here.

These preliminary results show that the latitude and seasonal dependences of the CHEM2D-H2O parameterization can offer an improved 10-day forecast of upper mesospheric water vapor compared to the 1-D parameterization currently used in some operational NWP/DA systems. We are now carrying out a more formal evaluation of middle atmospheric H_2O prognostic skill in NOGAPS-ALPHA over a longer time period using the fully coupled NWP/DA system, which will provide a more complete

and objective assessment of CHEM2D-H2O performance. Future work will combine NOGAPS-ALPHA prognostic H_2O and temperature fields in order to predict supersaturation conditions that lead to the formation of polar mesospheric clouds.

The CHEM2D-H2O parameterization is freely available for research purposes. For more details, please contact the lead author.

Acknowledgements. The authors thank S. D. Eckermann for valuable comments and discussion. We also wish to thank the EOS Aura MLS team and the TIMED SABER team. This work was supported by a grant from the Office of Naval Research. NOGAPS-ALPHA simulations were made possible by a grant of computer time from the DoD High Performance Computing Modernization Program at the US Air Force Research Laboratory.

References

Brasseur, G. and Solomon, S.: Aeronomy of the Middle Atmosphere, 2nd ed., D. Reidel, Norwell MA, USA, 452 pp., 1986. 14004, 14005

Coy, L., Allen, D. R., Eckermann, S. D., McCormack, J. P., Stajner, I., and Hogan, T. F.: Effects of model chemistry and data biases on stratospheric ozone assimilation, Atmos. Chem. Phys., 7, 2917–2935, 2007, http://www.atmos-chem-phys.net/7/2917/2007/. 14010, 14012

European Center for Medium-Range Weather Forecasts Integrated Forecast System Documentation Cy31r1, Part IV: Physical Processes, available at: http://www.ecmwf.int/research/ifsdocs/CY31r1/PHYSICS/IFSPart4.pdf, 2007. 14004, 14005

Feist, D. G., Geer, A. J., Müller, S., and Kämpfer, N.: Middle atmosphere water vapour and dynamical features in aircraft measurements and ECMWF analyses, Atmos. Chem. Phys., 7, 5291–5307, 2007, http://www.atmos-chem-phys.net/7/5291/2007/. 14004, 14015

Froidevaux, L., Livesey, N. J., Read, W. G., et al.: Early validation analyses of atmospheric profiles from EOS MLS on the Aura satellite, IEEE T. Geosci. Remote Sens., 44, 1106–1121, 2006. 14007, 14012

Garcia, R. R., Marsh, D. R., Kinnison, D. E., Boville, B. A., and Sassi, F.: Simulation of secular trends in the middle atmosphere, J. Geophys. Res., 112, D09301, doi:10.1029/2006JD007485, 2007. 14007

Geer, A. J., Lahoz, W. A., Jackson, D. R., Cariolle, D., and McCormack, J. P.: Evaluation of linear ozone photochemistry parametrizations in a stratosphere-troposphere data assimilation

system, Atmos. Chem. Phys., 7, 939–959, 2007, http://www.atmos-chem-phys.net/7/939/2007/. 14010

Grooß, J.-U. and Russell, J. M.: Technical note: A stratospheric climatology for O_3, H_2O, CH_4, NO_x, HCl and HF derived from HALOE measurements, Atmos. Chem. Phys., 5, 2797–2807, 2005, http://www.atmos-chem-phys.net/5/2797/2005/. 14006, 14010

Hogan, T. and Rosmond, T.: The description of the Navy Operational Global Atmospheric Prediction System's spectral forecast model, Mon. Weather Rev., 119, 1186–1815, 1991. 14006

Hoppel, K. W., Baker, N. L., Coy, L., Eckermann, S. D., McCormack, J. P., Nedoluha, G., and Siskind, D. E.: Assimilation of stratospheric and mesospheric temperatures from MLS and SABER into a global NWP model, Atmos. Chem. Phys. Discuss., 8, 8455–8490, 2008, http://www.atmos-chem-phys-discuss.net/8/8455/2008/. 14006, 14007

Kutepov A. A., Feofilov, A. G., Marshall, B. T., Gordley, L. L., Pesnell, W. D., Goldberg, R. A., and Russell, J. M.: SABER temperature observations in the summer polar mesosphere and lower thermosphere: Importance of accounting for the CO_2 ν_2 quanta V-V exchange, Geophys. Res. Lett., 33, L21809, doi:10.1029/2006GL026591, 2006. 14007

Lambert, A., Read, W. G., Livesey, N. J., et al.: Validation of the Aura Microwave Limb Sounder middle atmospheric water vapor and nitrous oxide measurements, J. Geophys. Res., 112, D24S36, doi:10.1029/2007JD008724, 2007. 14015

Lahoz, W. A., Errera, Q., Swinbank, R., and Fonteyn, D.: Data assimilation of stratospheric constituents: A review, Atmos. Chem. Phys., 7, 5745–5773, 2007, http://www.atmos-chem-phys.net/7/5745/2007/. 14008

LeTexier, H., Solomon, S., and Garcia, R. R.: the role of molecular hydrogen and methane oxidation in the water vapour budget of the stratosphere, Q. J. R. Meteorol. Soc., 114, 281–295, 1988. 14002, 14004

McCormack, J. P., Eckermann, S. D., Coy, L., et al.: NOGAPS-ALPHA model simulations of stratospheric ozone during the SOLVE2 campaign, Atmos. Chem. Phys., 4, 2401–2423, 2004, http://www.atmos-chem-phys.net/4/2401/2004/. 14001

McCormack, J. P., Eckermann, S. D., Siskind, D. E., and McGee, T. J.: CHEM2D-OPP: A new linearized gas-phase ozone photochemistry parameterization for high-altitude NWP and climate models, Atmos. Chem. Phys., 6, 4943–4972, 2006, http://www.atmos-chem-phys.net/6/4943/2006/. 14001, 14002, 14006, 14007, 14008, 14010

McCormack, J. P., Siskind, D. E., and Hood, L. L.: Solar-QBO interaction and its impact on

stratospheric ozone in a zonally averaged photochemical transport model of the middle atmosphere, J. Geophys. Res., 112, D16109, doi:10.1029/2006JD008369, 2007. 14002

Nedoluha, G., Bevilacqua, R., Gomez, R., Siskind, D., Hicks, B., Russell, J., and Connor, B.: Increases in middle atmospheric water vapor as observed by the Halogen Occultation Experiment and the ground-based Water Vapor Millimeter-wave Spectrometer from 1991–1997, J. Geophys. Res., 103, D3, 3531–3543, 1998. 14016

Peng, M. S., Ridout, J. A., and Hogan, T. F.: Recent modifications of the Emanuel convective scheme in the Navy Operational Global Atmospheric Prediction System, Mon. Weather Rev., 132, 1254–1268, 2004. 14006

Randel, W. J., Wu, F., Russel, J. M., Roche, A., and Waters, J. W.: Seasonal cycles and QBO variations in stratospheric CH_4 and H_2O observed in UARS HALOE data, J. Atmos. Sci., 55, 163–185, 1998. 14004, 14006, 14010

Randel, W. J., Wu, F., Russell, J. M., and Waters, J.: Space-time patterns of trends in stratospheric constituents derived from UARS measurements, J. Geophys. Res., 104, D3, 3711–3727, 1999. 14016

Sander, S. P., Friedl, R. R., Ravishankara, A. R., et al.: Chemical kinetics and photochemical data for use in atmospheric studies, Evaluation No. 14, Jet Propulsion Laboratory, Pasadena CA, USA, 2003. 14002

Siskind, D. E., Eckermann, S. D., McCormack, J. P., et al.: Hemispheric differences in the temperature of the summertime stratosphere and mesosphere, J. Geophys. Res., 108, D2, 4051, doi:10.1029/2002JD002095, 2003.

Slingo, J. M.: The development and verification of a cloud prediction scheme in the ECMWF model, Q. J. R. Meteorol. Soc., 113, 899–927, 1987. 14006

Teixeira, J. and Hogan, T.: Boundary layer clouds in a global atmospheric model: Simple cloud cover parameterization, J. Climate, 15, 1261–1276, 2002. 14006

Tiedtke, M.: The sensitivity of the time-scale flow to cumulus convection in the ECMWF model, Proceedings from the Workshop on Large-Scale Numerical Models, European Centre for Medium-Range Weather Forecasts, Reading, England, 28 November–1 December 1983, 297–316, 1984. 14006

Untch, A. and Simmons, A. J.: Increased stratospheric resolution in the ECMWF forecasting system, ECMWF Newsletter No. 82, available at: http://www.ecmwf.int/publications/newsletters/pdf/82.pdf, 1999. 14004

Table 1. H_2O photochemistry parameterizations used in the NOGAPS-ALPHA forecast model simulations.

Experiment Name	Description
EXP1	CHEM2D-H2O, r^o based on climatology
EXP2	CHEM2D-H2O, r^o based on June 2007 analyses
EXP3	ECMWF

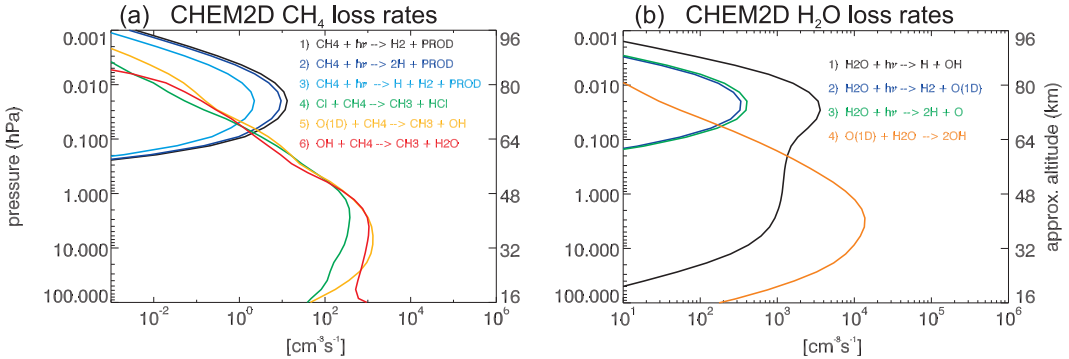

Fig. 1. Vertical profiles of the dominant CHEM2D model loss rates (molecules cm^{-3} s^{-1}) at 5° N on June 15 for **(a)** CH_4 and **(b)** H_2O.

ACPD
8, 13999–14032, 2008

Title Page
Abstract Introduction
Conclusions References
Tables Figures
◀I ▶I
◀ ▶
Back Close
Full Screen / Esc
Printer-friendly Version
Interactive Discussion

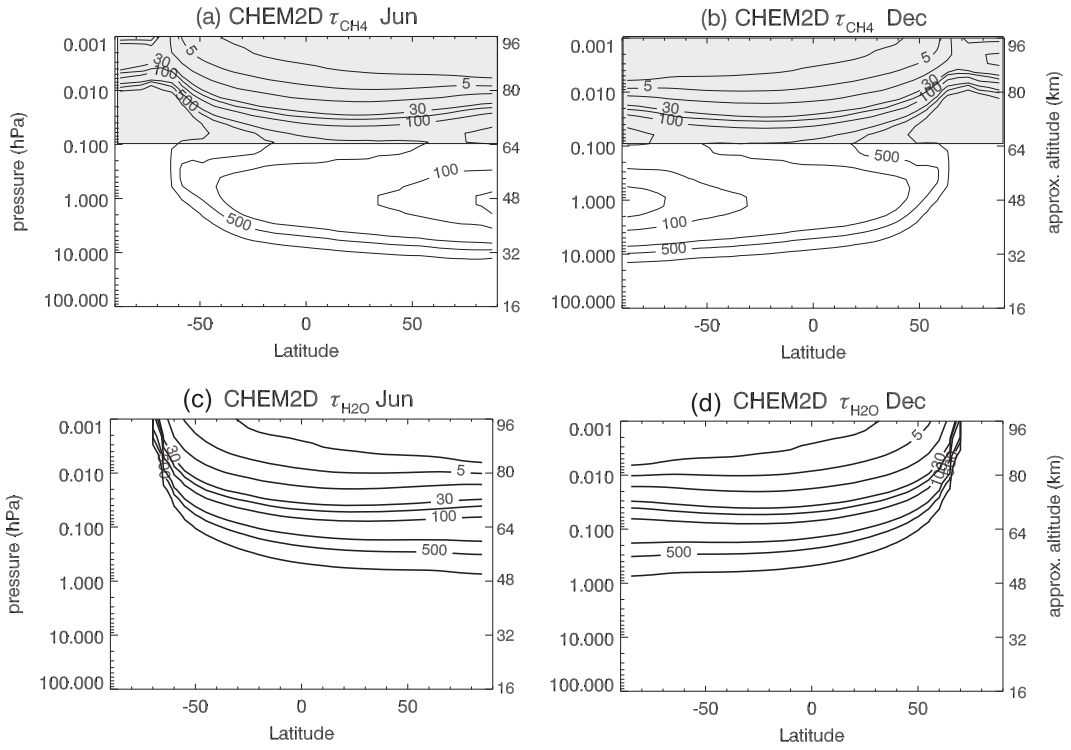

Fig. 2. Pressure-latitude plots of CHEM2D CH_4 photochemical lifetimes (in days) for **(a)** 15 June and **(b)** 15 December, and of CHEM2D H_2O lifetimes for **(c)** 15 June and **(d)** 15 December. Shading in (a) and (b) indicates region where CH_4 loss is primarily through photolysis. Contours are drawn at 3, 5, 10, 30, 50, 100, 300, 500, and 1 000 days.

ACPD
8, 13999–14032, 2008

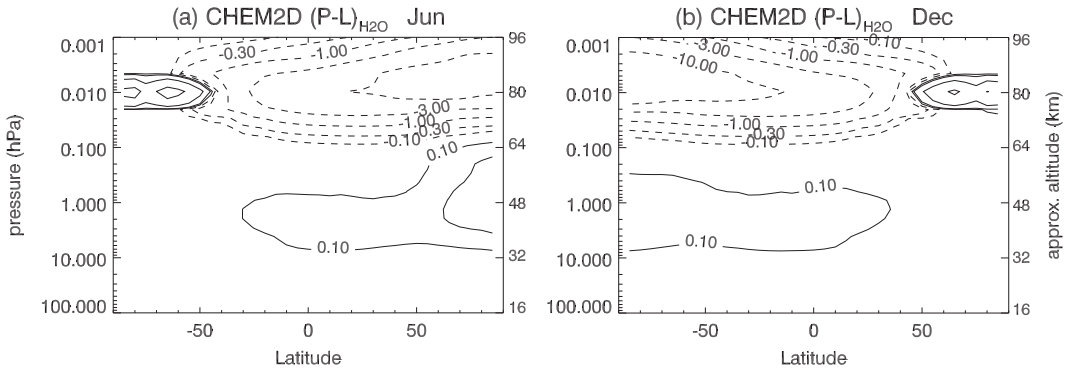

Fig. 3. Pressure-latitude plots of net CHEM2D middle atmosphere water vapor photochemical tendency $(P-L)_{H2O}$ for **(a)** 15 June and **(b)** 15 December in parts per million (volume) per month. Contours are drawn at ±0.1, ±0.3, ±1, ±3, and ±10 ppmv per month. Dashed contours denote negative values.

ACPD
8, 13999–14032, 2008

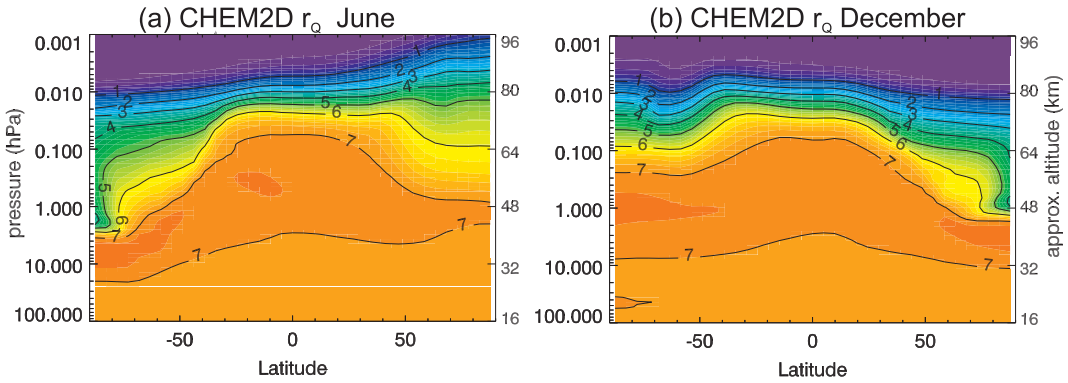

Fig. 4. Pressure-latitude plots of total hydrogen r_Q (in ppmv) from the CHEM2D model for **(a)** 15 June and **(b)** 15 December. Contours are drawn every 1 ppmv.

ACPD
8, 13999–14032, 2008

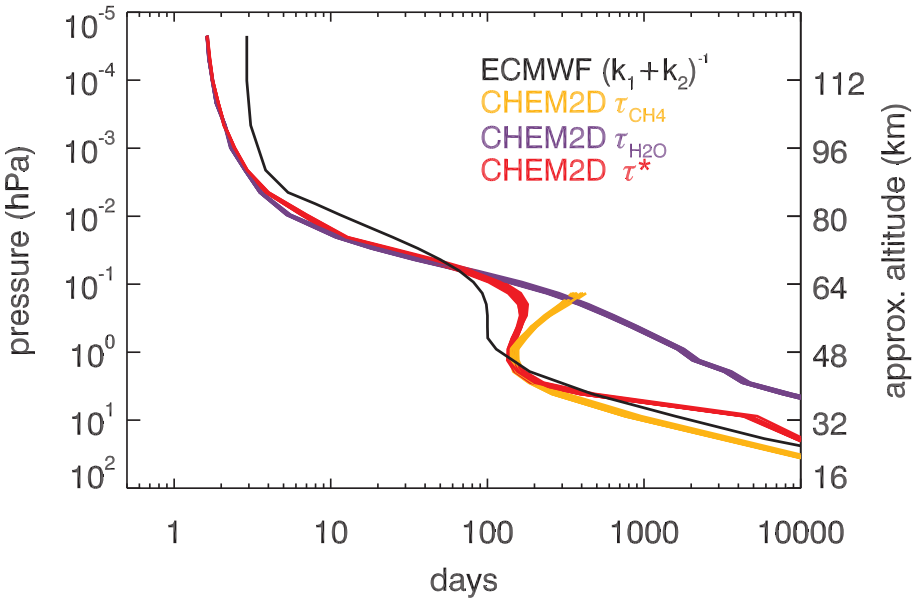

Fig. 5. Comparison of combined photochemical lifetime (days) in the ECMWF water vapor photochemistry parameterization (black curve) with CHEM2D lifetimes τ_{H2O} (purple curves), τ_{CH4} (gold curves), τ^* (red curves) for all 12 months over the equator. The CHEM2D τ_{CH4} profile is only plotted at levels where CH_4 oxidation is the dominant loss process (c.f., Fig. 1 and unshaded region in Fig. 2).

ACPD
8, 13999–14032, 2008

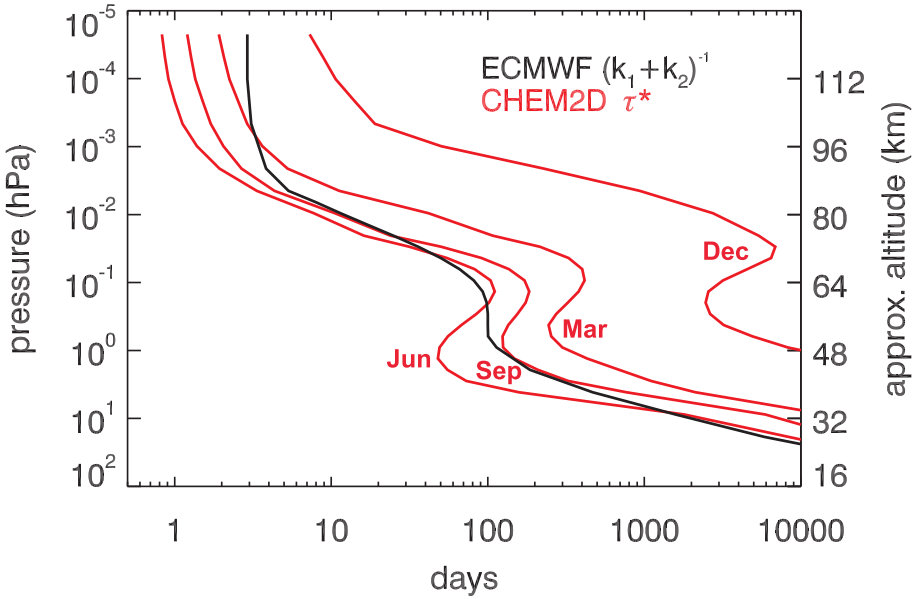

Fig. 6. Comparison of combined photochemical lifetime (days) in the ECMWF water vapor photochemistry parameterization (black curve) with values of the CHEM2D effective lifetime τ^* (red curves) at 70° N on the 15th day of March, June, September, and December.

ACPD
8, 13999–14032, 2008

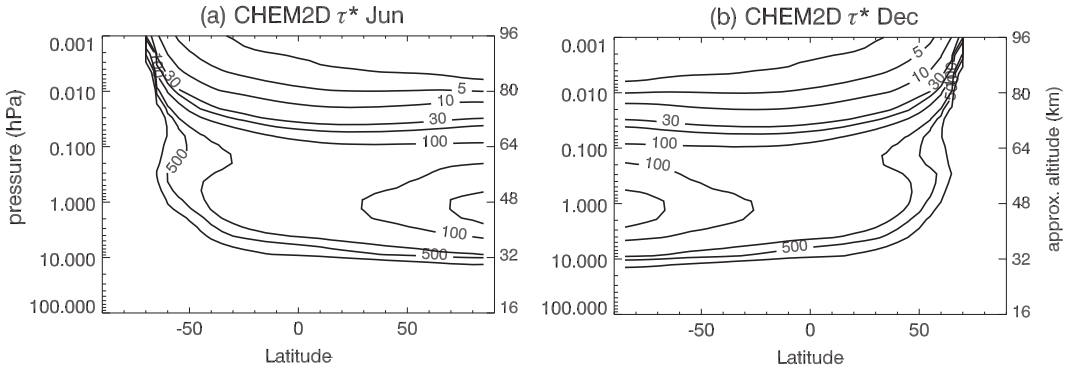

Fig. 7. Pressure-latitude plots of the effective photochemical lifetime τ^* (days) used in the CHEM2D-H2O parameterization for **(a)** 15 June and **(b)** 15 December.

ACPD
8, 13999–14032, 2008

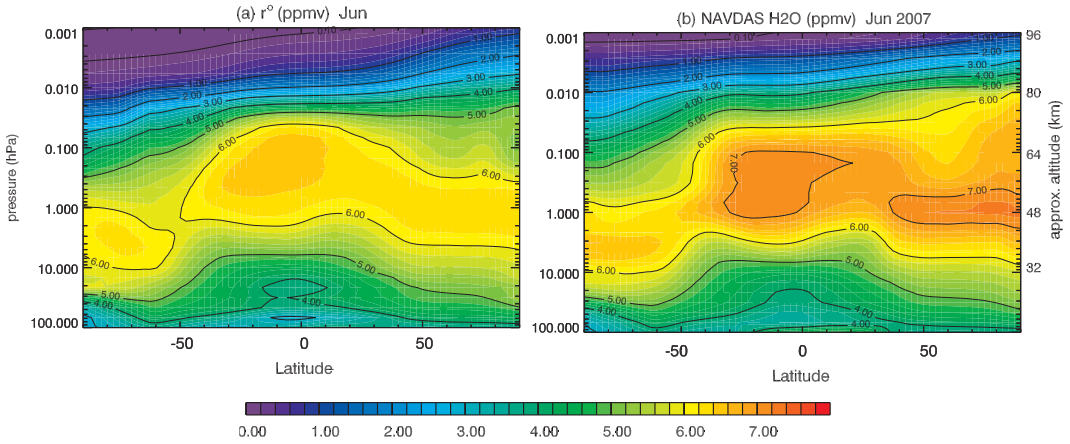

Fig. 8. Pressure-latitude plots of the zonal mean reference state H_2O mixing ratio r^o (in ppmv) for June based on **(a)** the combined UARS HALOE/MLS climatology used in EXP1 and **(b)** the June 2007 NOGAPS-ALPHA analyses of Aura MLS measurements used in EXP2.

ACPD
8, 13999–14032, 2008

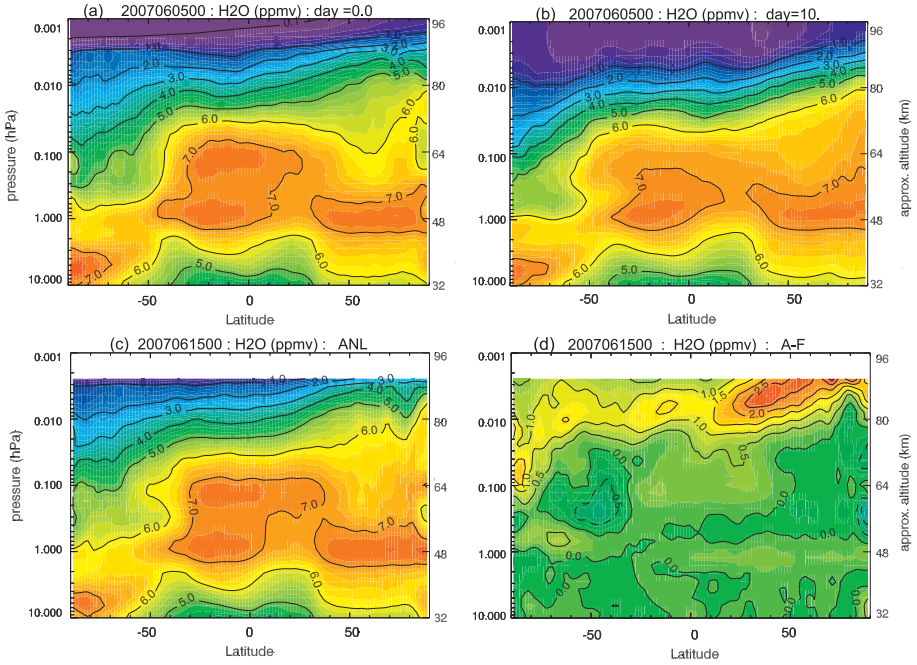

Fig. 9. Pressure-latitude plots of **(a)** NOGAPS-ALPHA analyzed zonal mean H_2O mixing ratios for 00:00 UTC 5 June 2007; **(b)** zonal mean forecast model H_2O mixing ratios at day 10 of the EXP1 model simulation initialized 00:00 UTC 5 June and valid 00:00 UTC 15 June 2007 **(c)** zonal mean NOGAPS-ALPHA analyzed H_2O at 00:00 UTC on 15 June 2007; **(d)** differences in H_2O mixing ratios between the 10-day forecast (F) in (b) and the analyzed (A) values in (c). Solid and dashed contours denote positive and negative differences, respectively.

ACPD
8, 13999–14032, 2008

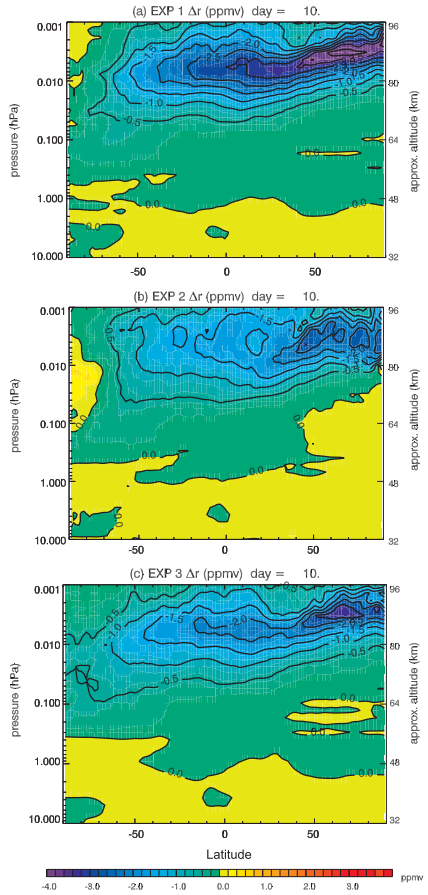

Fig. 10. Zonal mean values of Δr, the difference between NOGAPS-ALPHA model prognostic H_2O and passive (i.e., no photochemistry) H_2O on day 10 of the **(a)** EXP1, **(b)** EXP2, and **(c)** EXP3 simulations initialized 00:00 UTC 5 June 2007.

ACPD
8, 13999–14032, 2008

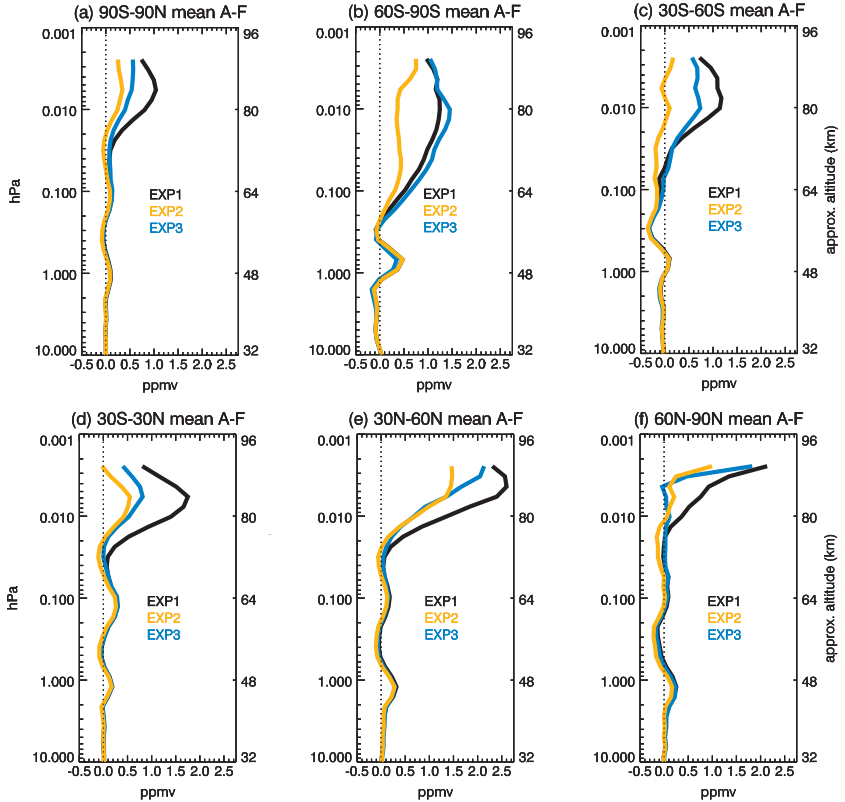

Fig. 11. Mean differences between NOGAPS-ALPHA analyzed H_2O and 10-day forecast H_2O (A–F) based on forecast model simulations initialized 00:00 UTC on June 5, 10, 15, 20, and 25, 2007 using CHEM2D-H2O with climatological reference state (EXP1), CHEM2D-H2O with analyzed reference state (EXP2), and the ECMWF parameterization (EXP3). Results are presented for **(a)** the global area-weighted average A–F, **(b)** 60° S–90° S, **(c)** 30° S–60° S, **(d)** 30° S–30° N, **(e)** 30° N–60° N, and **(f)** 60° N–90° N.

ACPD
8, 13999–14032, 2008

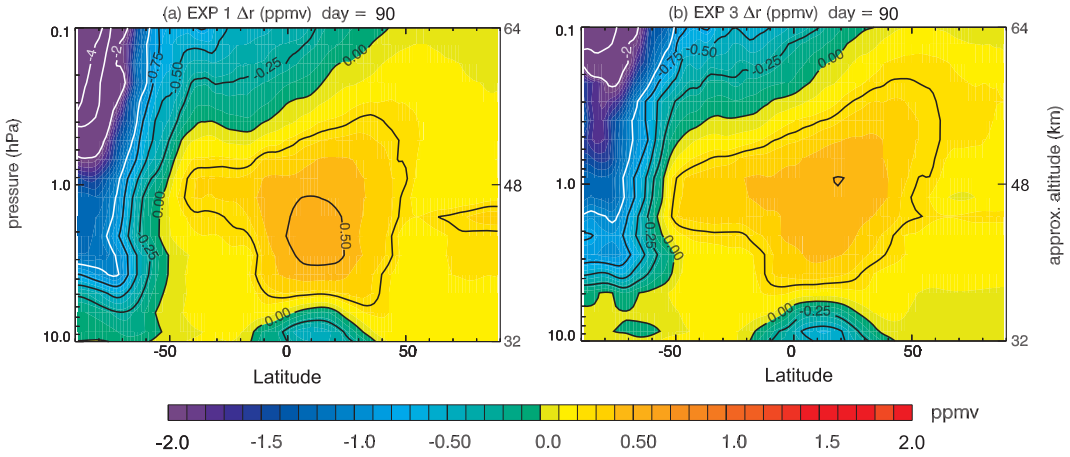

Fig. 12. Zonal mean values of the difference between NOGAPS-ALPHA prognostic H_2O and passive H_2O mixing ratio, Δr, on day 90 of **(a)** EXP1 and **(b)** EXP3 free-running NOGAPS-ALPHA forecast simulations initialized 00:00 UTC 5 June 2007.

ACPD
8, 13999–14032, 2008